Methodology for Analysis of Afterbodies for Three-Dimensional Aircraft Configurations

Eugene H. Miller*
Grumman Aircraft Systems, Bethpage, New York

Today's modern fighter design, with multifunction nozzles, is placing an increased emphasis on nozzle/airframe integration. The current tools available to the aircraft designer for aft-end design and evaluation are model test reports, being disseminated mainly by government laboratories, and three-dimensional numerical computation codes. Test data utilization usually is limited by the suitability of the area that has been tested. The second approach, analysis, usually requires time-consuming three-dimensional configuration data input. Recognizing the need for a quicker means of solution, useful in a preliminary design environment, a semiempirical computer methodology for determining three-dimensional aircraft afterbody performance has been developed. The essence of the approach is to construct equivalent bodies of revolution of three-dimensional bodies and then to utilize a straight or hybrid axisymmetric analysis. This approach has been developed for single- and twin-engine axisymmetric and two-dimensional afterbodies. The methodology has been verified by comparisons of afterbody drag and axial and longitudinal pressure distributions.

Nomenclature

$\mathcal{R}$ = aspect ratio
C_D = drag coefficient
C_f = friction coefficient
C_L = lift coefficient
D = diameter
L = length
M = Mach number
MB = metric break
P = pressure
R = radius
V = velocity
W = width
X = length
δ = boundary-layer height
θ = momentum thickness
μ = viscosity
ρ = density

Subscripts

n = nozzle
s = static

Introduction

THE aft-end of military aircraft historically has contributed a significant portion, sometimes almost half,[1] of the overall aircraft drag (see Fig. 1). This is the result of the complexities introduced into aircraft/powerplant design as military aircraft configurations evolved from simple single-engine nonafterburning jet aircraft of the early 1950's to today's complex twin-engine aircraft with multifunction nozzles.

The first modification to the nozzle design occurred with the incorporation of an afterburner. This required a significant increase in nozzle throat area to accommodate the high-temperature exhaust gases. The resulting configuration either had a large boattail angle (for nonafterburner operation) with the possibilities of flow separation on the afterbody, or internal duct variations with accompanying base drag penalties.

The next step in the design evolution incorporated variable nozzle exit area in axisymmetric convergent-divergent (C-D) nozzles in order to optimize internal thrust. This required an assessment of the boattail drag changes with engine power setting.

Aircraft also evolved from single- to twin-engine jet fighters for increased reliability, weapons carriage, and other requirements. This produced configurations with "dirty" flowfields caused, for example, by "guttering" between the nacelles or by booms. Future multirole military aircraft designs will incorporate multifunction nozzles, as shown in Fig. 2,[2] with thrust reversing and thrust vectoring effects, which must be accounted for in propulsion system performance calculations. Two-dimensional nozzle designs have evolved to accommodate the multifunction nozzle requirements[3,4] and eliminate guttering; they dominate today's technology studies.

To permit analytic performance prediction of the evolving designs, a steady progression of analytical techniques has developed. Initially, the single-engine fighter required an axisymmetric flowfield analysis with accompanying viscous exhaust-plume and boundary-layer effects. External flow separation criteria were also needed to assess the effect of variable nozzle boattail angles. Thus, the interference effects of the exhaust system upon the afterbody could be taken into account. Analytical codes were developed to perform these calculations.[5,6] Current improvements in these codes generally are aimed at reduction in computer run time.[7,8]

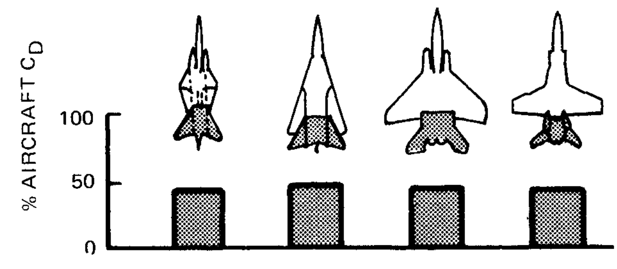

Fig. 1 Comparison of subsonic aft-end drag for several aircraft, $C_L = 0$.

Received July 24, 1987; revision received Aug. 27, 1987.

*Engineering Specialist, Propulsion.

The advent of twin-engine fighters produced a fully three-dimensional flowfield around the afterbody that is not currently amenable to rapid analysis. Three-dimensional codes such as VSAERO[9] and ARC3D[10] currently are disseminated to industry and are being exercised. However, their input requirements, fully defining the afterbody contours, necessitate extensive geometric definition. Analytical problems have been complicated further by the introduction of two-dimensional nozzles. The simpler flowfield codes were able to perform either axisymmetric or infinite-aspect-ratio two-dimensional flowfield calculations; now analytical tools capable of analyzing finite-aspect-ratio two-dimensional nozzles are required.

Methodologies have been devised to address rapid calculation of these two areas: three-dimensional twin-engine afterbodies with axisymmetric nozzles and three-dimensional twin-engine afterbodies with two-dimensional nozzles. The calculation procedures are described subsequently.

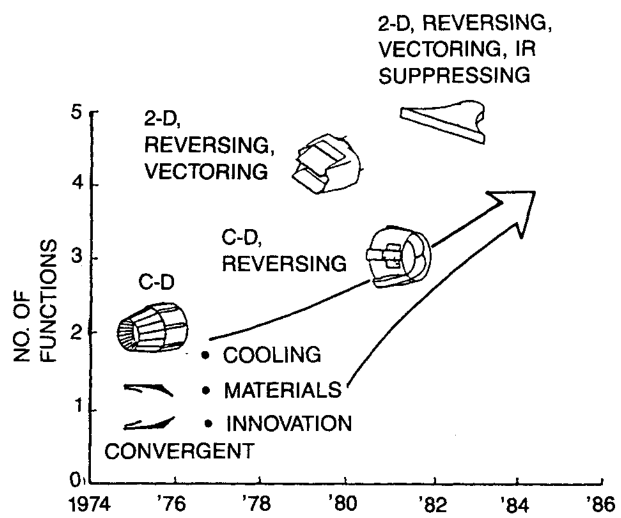

Fig. 2 Trends in nozzle technology.

Axisymmetric Nozzle Methodology

For the axisymmetric nozzle aircraft configuration, it was postulated that the aircraft afterbody area distribution be converted into an equivalent body of revolution, thereby eliminating the three-dimensional effects such as guttering and local bumps, combining these effects in the area distribution. A similar approach has been applied in the past with the "coke-bottle" effect for supersonic flow.

The axisymmetric nozzle/afterbody approach begins with the construction of an equivalent body of revolution (EBR) of the afterbody (aft-end minus empennage) configuration to be analyzed. That is, the actual cross-sectional area distribution of the afterbody as a function of fuselage station is converted into equivalent-area circles, and the circle radius vs station data for the equivalent circles becomes the radius vs length function for an EBR of the afterbody. These data provide the geometry input parameters for the numerical code, GAC-BOAT,[5,6] utilized for this study. This methodology is depicted in Fig. 3.

As shown in this figure, the geometric distribution, together with external flowfield properties such as Mach number, Reynolds number, friction coefficient, displacement, and momentum thickness and the exhaust nozzle exit properties (such as exit angle, static pressure, and Mach number) comprise the input for the computer code.

The methodology and results for twin-engine aircraft are depicted in Figs. 4–9. The configurations examined include an F-18 scale model and a NASA research model.

The F-18 scale model tested at NASA Langley[11] is shown in Fig. 4; the area analyzed downstream of the metric break (M.B.) station is shown crosshatched. The empennage surfaces were removed and an EBR of the afterbody was constructed from the remaining cross-sectional area (Fig. 5). A comparison of the test data and analytic code results is shown in Fig. 6. Afterbody drag coefficient (based on A_{wing}) is plotted against Mach number. The scale-model empennage drag was removed from the test data to compare the "clean" test model and analytic results, which also excluded the empennage. It is seen that good agreement is obtained in the Mach number range of 0.80–1.20. There appears to be a significant discrepancy between the test and analytic data in the Mach 0.60 region. There is also a larger decrease in afterbody drag with Mach

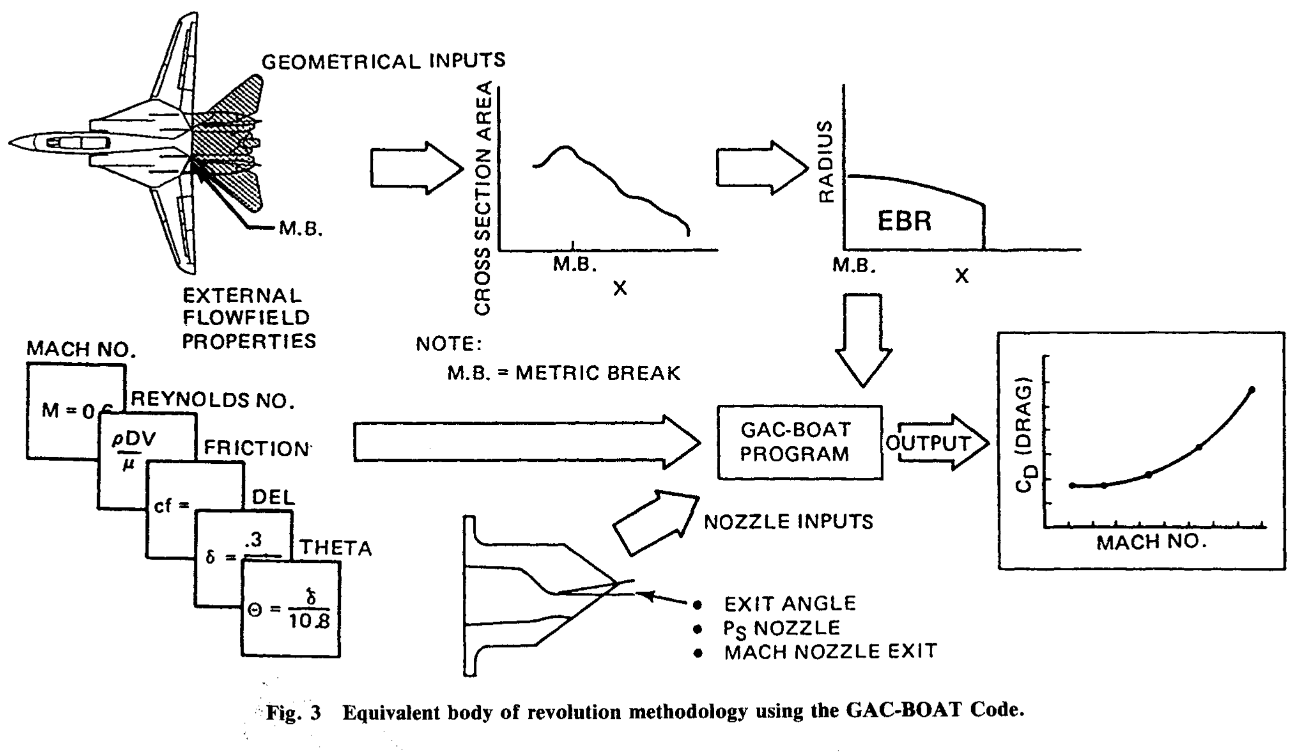

Fig. 3 Equivalent body of revolution methodology using the GAC-BOAT Code.

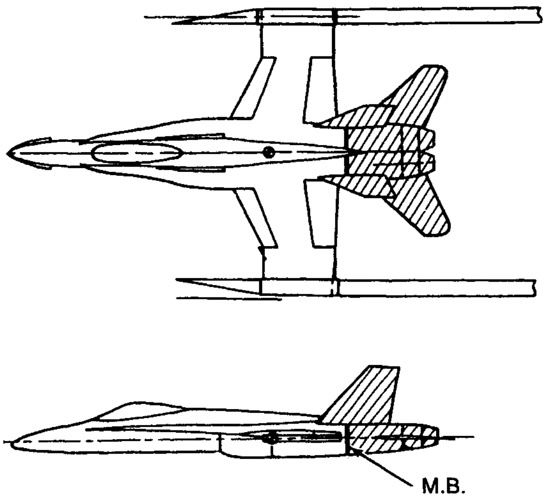

Fig. 4 F-18 wind tunnel model.

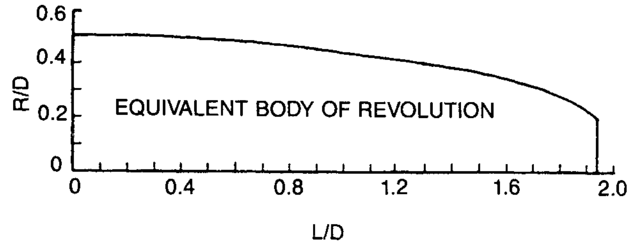

Fig. 5 F-18 afterbody radius vs length.

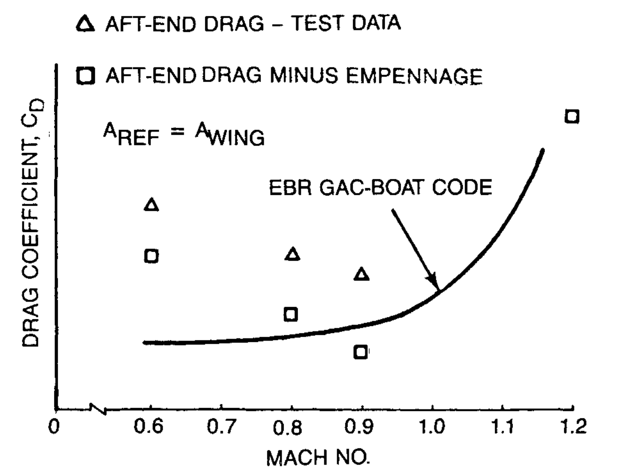

Fig. 6 Comparison of NASA test data with GAC-BOAT code force data for F-18 afterbody.

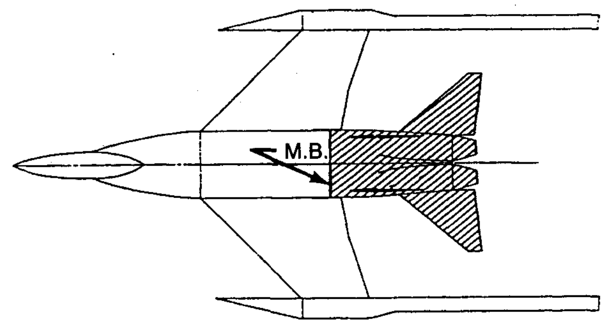

Fig. 7 NASA research wind tunnel model.

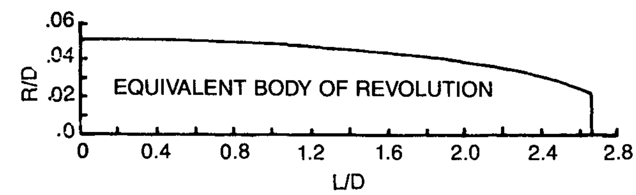

Fig. 8 NASA research model afterbody radius vs length.

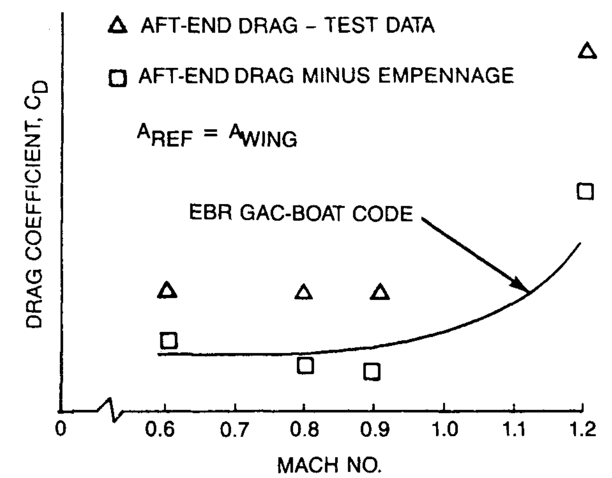

Fig. 9 Comparison of NASA test data with GAC-BOAT code force data for NASA research model afterbody.

number for the test data than is usually experienced. These results might be due to Reynolds number effects and/or local flow separation along the afterbody. The GAC-BOAT results go against the general trend of a slight drag decrease subsonically, before the drag rise; they display a minimal drag increase.

The technique was also applied to an advanced NASA research model,[12] shown in Fig. 7; the area analyzed is again depicted crosshatched. The EBR of the afterbody is shown in Fig. 8. The test data and analytic comparison of afterbody drag coefficients are presented in Fig. 9. A very good correlation of test data and analytic results was obtained in this case.

Two-Dimensional Nozzle Methodology

The GAC-BOAT program originally performed axisymmetric and infinite-aspect-ratio two-dimensional calculations. Two-Dimensional nozzle contours, analyzed using the infinite-aspect-ratio two-dimensional flowfield calculation, were used to generate the pressure distributions on the upper and lower surfaces. This distribution was then pressure-area-integrated over the actual finite-aspect-ratio upper and lower surfaces to determine the resultant external nozzle pressure forces. Because this approach was found to lack correlation with many two-dimensional test applications, the GAC-BOAT program was modified to include an optional hybrid calculation procedure for these nozzles.

The hybrid approach for two-dimensional nozzles employs axisymmetric flowfield pressure distribution solutions, generated from bodies defined by the actual upper and lower afterbody contours. (This approach assumes no sidewall boattail.) These pressure distributions are then pressure-area-integrated over their upper and lower, finite-aspect-ratio, two-dimensional surfaces. Nozzle sidewall and upper and lower surface external skin-friction forces are also calculated and included in resultant external force calculations.

The rationale for this methodology is based on comparisons of analytic and test data along two directions on the afterbody. The first is a comparison of the longitudinal pressure distribution along a finite-aspect-ratio two-dimensional afterbody. The second examines the lateral pressure distribution on the two-dimensional afterbody.

The longitudinal pressure distributions examined were for two-dimensional nacelles of an air-to-surface (ATS) aircraft configuration designed for a supersonic strike mission.[13] The data examined was for 2-D C-D nozzles with aspect ratios (Æ) of 3.6 and 7.0. The Æ = 3.6 comparisons are shown in Fig. 10. It can be seen that the GAC-BOAT code closely follows the nacelle centerline test data by matching the expansion pressure coefficient level of −0.2 and duplicating the recompression over most of the nozzle. There is some discrepancy near the nozzle trailing edge. The two-dimensional infinite-aspect-ratio solution produced an expansion level much too low (larger negative C_p). The Æ = 7.0 comparison is shown in Fig. 11. The initial expansion pressure distribution on the nacelle centerline is fairly well matched. Excellent agreement was also attained for the nozzle recompression. Again, the two-dimensional infinite-aspect-ratio solution produced a much too negative pressure coefficient. Therefore, these data showed that a generally good agreement in longitudinal pressure distribution along a two-dimensional nacelle/nozzle can be achieved by use of an axisymmetric pressure distribution at aspect ratios in the range of typical afterbody nacelle design.

The second rationale for the methodology, that of reasonable uniformity of transverse pressure distribution across the nacelle, is demonstrated in Fig. 12. These data were taken from a two-dimensional model (configuration 2, Mach no. = 0.90) tested at NASA Langley.[14] It can be seen that, over a significant portion of the afterbody, the centerline pressure distribution is valid.

Finally, the hybrid approach was verified by comparing analytic and test drag results. The test data utilized was once

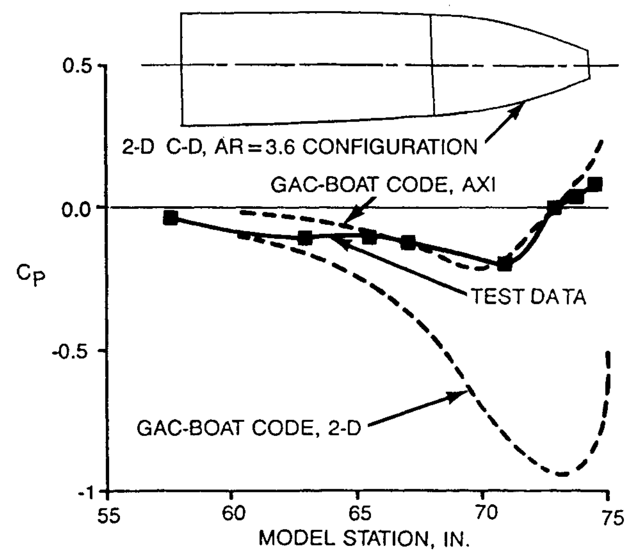

Fig. 10 Pressure distribution for ATS configuration, cruise nozzle, Æ = 3.6, Mach no. = 0.90.

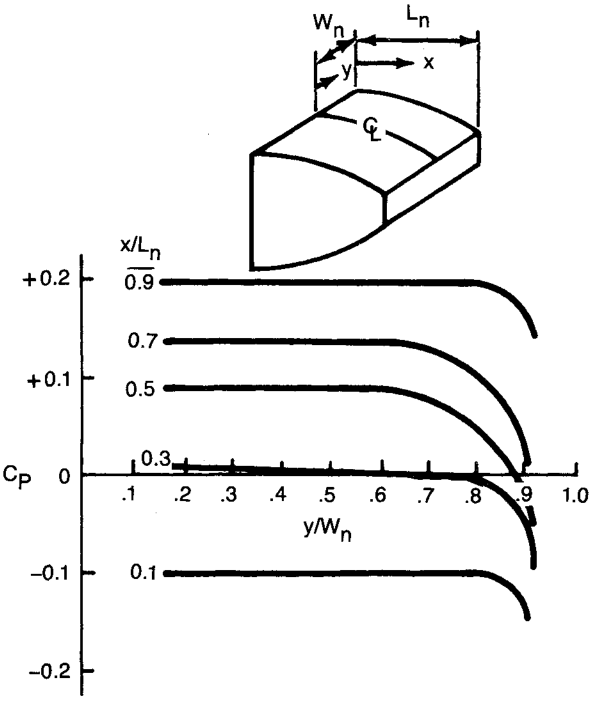

Fig. 12 Transverse pressure distribution, Mach no. = 0.90.

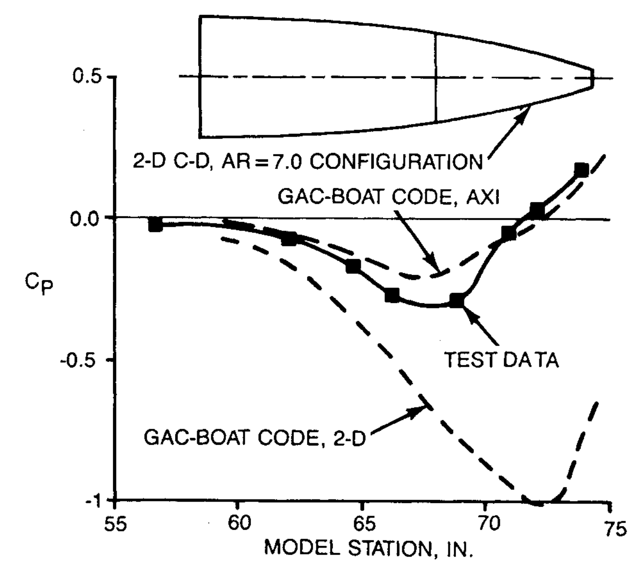

Fig. 11 Pressure distribution for ATS configuration, cruise nozzle, Æ = 7.0, Mach no. = 0.90.

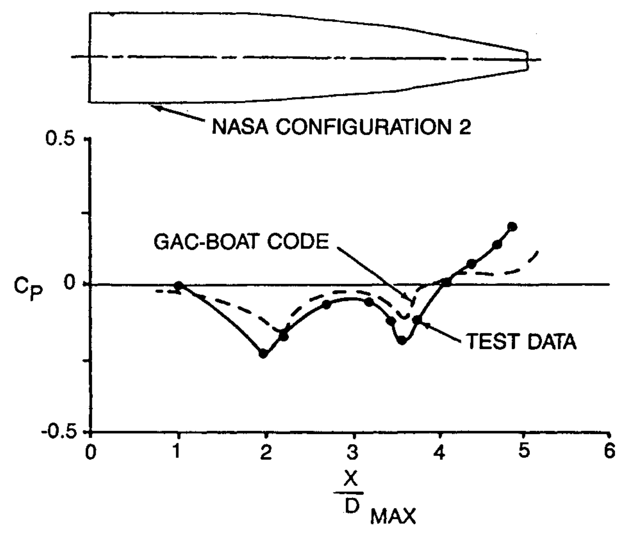

Fig. 13 NASA test data vs GAC-BOAT code pressure distribution for two-dimensional nozzle/afterbody configuration, NPR = 5.0, Mach no. = 0.90.

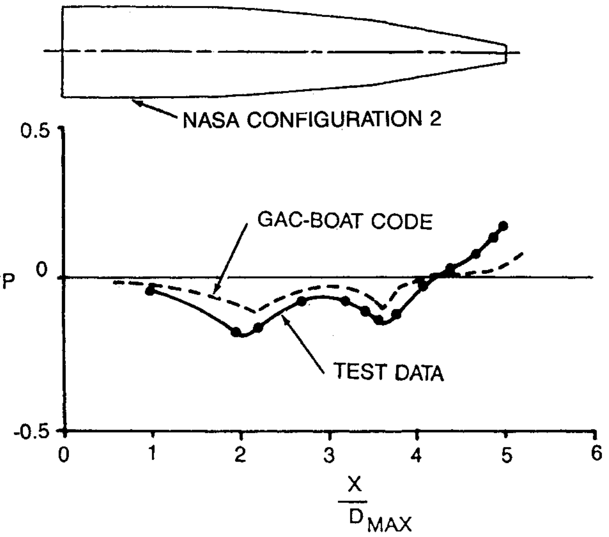

Fig. 14 NASA test data vs GAC-BOAT code pressure distribution for 2-D nozzle/afterbody configuration, NPR = 3.5, Mach no. = 0.60.

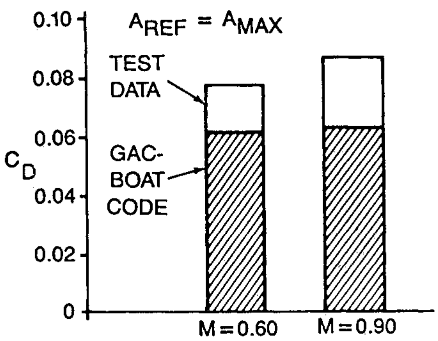

Fig. 15 NASA test data vs GAC-BOAT code force data for 2-D nozzle/afterbody configuration.

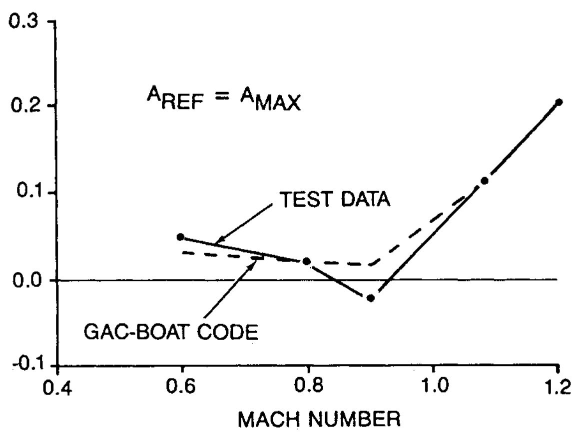

Fig. 16 Afterbody drag for F-18 configuration, 2-D C-D cruise nozzle, spacing ratio = 1.08, area ratio = 1.15.

again for the NASA Langley model (configuration 2) of Ref. 14. The centerline pressure distribution comparison for this model at a Mach number of 0.90 and a nozzle pressure ratio (NPR) of 5.0 is shown in Fig. 13. It can be seen that the GAC-BOAT code correctly follows the nacelle/nozzle pressure distribution, picking up the two expansions—the first on the nacelle and the second on the nozzle. The GAC-BOAT nozzle pressure recovery falls below the test data, but a

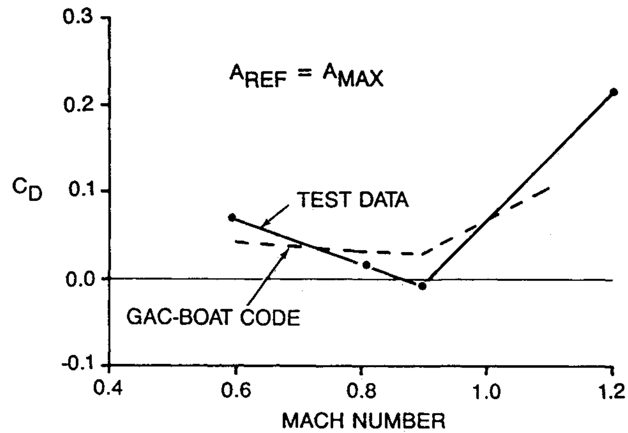

Fig. 17 Afterbody drag for F-18 configuration, 2-D C-D cruise nozzle, spacing ratio = 1.08, area ratio = 1.65.

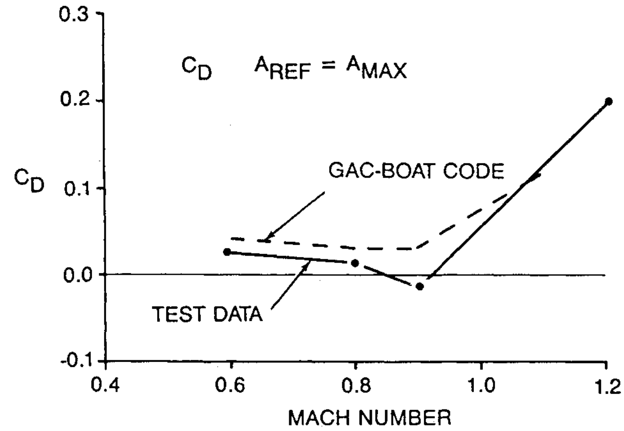

Fig. 18 Afterbody drag for F-18 configuration, 2-D SERN cruise nozzle, spacing ratio = 1.08, area ratio = 1.15.

definite recompression is observed. Similar results are shown in Fig. 14 for the same configuration run at a Mach number of 0.60 and NPR of 3.5. The drag results are shown in Fig. 15. The afterbody drag coefficient (based on A_{max} of the EBR) is shown for the NASA and GAC-BOAT results for Mach numbers of 0.60 and 0.90. It can be seen that the methodology does a reasonable job of replicating the drag values.

The methodology applied to a twin-nacelle two-dimensional body[11] is shown in Figs. 16 and 17 for 2-D C-D nozzles of area ratios of 1.15 and 1.65. It can be seen that a good agreement of afterbody drag coefficient (based on the EBR A_{max}) vs Mach number occurs for both configurations.

The next configuration examined was a single-expansion ramp nozzle (SERN). The same basic two-dimensional hybrid methodology was applied. However, for the SERN nozzle, separate calculations of pressure distribution were performed for the upper and lower nozzle surfaces. These pressures were then utilized to obtain the pressure drags of the two surfaces. Friction drag for these surfaces, together with the pressure drag, were combined with sidewall friction to provide the overall drag. Afterbody drag coefficients for the SERN nozzle on the same aircraft configuration are shown in Fig. 18.

Conclusions

A methodology has been established and verified for the calculation of afterbody drag on single- and twin-engine axisymmetric and two-dimensional afterbodies. This approach for afterbody drag calculation requires:

1) Construction of an equivalent body of revolution and

the calculation of an axisymmetric pressure distribution and subsequent axisymmetric integration to establish the drag for axisymmetric single- and twin-engine aircraft afterbodies.

2) Use of a hybrid methodology that performs axisymmetric calculations to establish the pressure distribution, and subsequent two-dimensional integration to establish the drag for two-dimensional single- and twin-engine aircraft afterbodies.

The methodology results in a rapid solution of afterbody drag of sufficient accuracy for the preliminary design environment.

References

[1]Capone, F. J., "The Nonaxisymmetric Nozzle—It Is for Real" AIAA Paper 79-1810, Aug. 1979.

[2]Richey, G. K., Surber, L. E., and Berrier, B. L., "Airframe–Propulsion Integration for Fighter Aircraft," AIAA Paper 83-8084, Jan. 1983.

[3]Miller, E., "Performance of a Forward Swept Wing Fighter Utilizing Thrust Vectoring and Reversing," *Journal of Aircraft*, Vol. 23, Jan. 1986, pp. 68–75.

[4]Miller, E. and Protopapas, J., "Nozzle Design and Integration in an Advanced Supersonic Fighter," *International Journal of Turbo and Jet Engines*, Vol. 2, No. 4, 1984, pp. 273–284.

[5]Davis, W. H. Jr., "Analysis of Isolated Subsonic-Transonic Boattails in the Presence of Separation and Exhaust Plume Entrainment," Grumman Aircraft Systems, Bethpage, NY, Propulsion Rept. PXP-001-55, Sept. 1978.

[6]August, R. A., "Analysis of Isolated Supersonic Boattails Including Plume and Viscosity Effects," Grumman Aircraft Systems, Bethpage, NY, Propulsion Rept. PXP-001-56, July 1980.

[7]Volpe, G., "Prediction of the Flow Over Supercritical High Lift Configurations by a Multi-Grid Algorithm," AIAA Paper 84-1664, June 1984.

[8]Volpe, G., "Multi-Grid Approximate Factorization Scheme for Two-Element Airfoil Flows," *AIAA Journal*, Vol. 25, June 1987, pp. 784–791.

[9]Maskow, B., "Program VSAERO, A Computer Program for Calculating the Nonlinear Aerodynamic Characteristics of Arbitrary Configurations," Analytic Methods, Inc., Redmond, WA, July 1983.

[10]Pulliam, T. and Steger, J., "Implicit Finite-Difference Simulations of 3-D Compressible Flow," *AIAA Journal*, Vol. 18, Feb. 1980, pp. 159–167.

[11]Capone, F. J., "Aeropropulsive Characteristics at Mach Numbers up to 2.2 of Axisymmetric and Nonaxisymmetric Nozzles Installed on an F-18 Model," NASA TP-2044, Aug. 1983.

[12]Bare, A. E. and Leavitt, L. D., "Effects of Twin-Vertical Tail Parameters on Twin Engine Afterbody/Nozzle Aerodynamic Characteristics," NASA TP-2158, May 1983.

[13]Hiley, P. E. et al., "Advanced Nozzle Concepts Program, Volume II—Nozzle Integration for Supersonic Strike Fighter Application," AFWAL TR-81-3165, April 1982.

[14]Pendergraft, O. C., Burley, J. R., and Bare, E. A., "Parametric Study of Afterbody/Nozzle Drag on Twin Two-Dimensional Convergent-Divergent Nozzles at Mach Numbers from 0.60 to 1.20," NASA TP-2640, Oct. 1986.